

Search for Quark-Lepton Compositeness and a Heavy W' Boson Using the $e\nu$ Channel in $p\bar{p}$ Collisions at $\sqrt{s} = 1.8$ TeV

(August 15, 2018)

T. Affolder,²³ H. Akimoto,⁴⁵ A. Akopian,³⁷ M. G. Albrow,¹¹ P. Amaral,⁸ D. Amidei,²⁵ K. Anikeev,²⁴ J. Antos,¹ G. Apollinari,¹¹ T. Arisawa,⁴⁵ A. Artikov,⁹ T. Asakawa,⁴³ W. Ashmanskas,⁸ F. Azfar,³⁰ P. Azzi-Bacchetta,³¹ N. Bacchetta,³¹ H. Bachacou,²³ S. Bailey,¹⁶ P. de Barbaro,³⁶ A. Barbaro-Galtieri,²³ V. E. Barnes,³⁵ B. A. Barnett,¹⁹ S. Baroiant,⁵ M. Barone,¹³ G. Bauer,²⁴ F. Bedeschi,³³ S. Belforte,⁴² W. H. Bell,¹⁵ G. Bellettini,³³ J. Bellinger,⁴⁶ D. Benjamin,¹⁰ J. Bensinger,⁴ A. Beretvas,¹¹ J. P. Berge,¹¹ J. Berryhill,⁸ A. Bhatti,³⁷ M. Binkley,¹¹ D. Bisello,³¹ M. Bishai,¹¹ R. E. Blair,² C. Blocker,⁴ K. Bloom,²⁵ B. Blumenfeld,¹⁹ S. R. Blusk,³⁶ A. Bocci,³⁷ A. Bodek,³⁶ W. Bokhari,³² G. Bolla,³⁵ Y. Bonushkin,⁶ D. Bortoletto,³⁵ J. Boudreau,³⁴ A. Brandl,²⁷ S. van den Brink,¹⁹ C. Bromberg,²⁶ M. Brozovic,¹⁰ E. Brubaker,²³ N. Bruner,²⁷ E. Buckley-Geer,¹¹ J. Budagov,⁹ H. S. Budd,³⁶ K. Burkett,¹⁶ G. Busetto,³¹ A. Byon-Wagner,¹¹ K. L. Byrum,² S. Cabrera,¹⁰ P. Calafiura,²³ M. Campbell,²⁵ W. Carithers,²³ J. Carlson,²⁵ D. Carlsmith,⁴⁶ W. Caskey,⁵ A. Castro,³ D. Cauz,⁴² A. Cerri,³³ A. W. Chan,¹ P. S. Chang,¹ P. T. Chang,¹ J. Chapman,²⁵ C. Chen,³² Y. C. Chen,¹ M. -T. Cheng,¹ M. Chertok,⁵ G. Chiarelli,³³ I. Chirikov-Zorin,⁹ G. Chlachidze,⁹ F. Chlebana,¹¹ L. Christofek,¹⁸ M. L. Chu,¹ Y. S. Chung,³⁶ C. I. Ciobanu,²⁸ A. G. Clark,¹⁴ A. Connolly,²³ J. Conway,³⁸ M. Cordelli,¹³ J. Cranshaw,⁴⁰ R. Cropp,⁴¹ R. Culbertson,¹¹ D. Dagenhart,⁴⁴ S. D'Auria,¹⁵ F. DeJongh,¹¹ S. Dell'Agnello,¹³ M. Dell'Orso,³³ L. Demortier,³⁷ M. Deninno,³ P. F. Derwent,¹¹ T. Devlin,³⁸ J. R. Dittmann,¹¹ A. Dominguez,²³ S. Donati,³³ J. Done,³⁹ M. D'Onofrio,³³ T. Dorigo,¹⁶ N. Eddy,¹⁸ K. Einsweiler,²³ J. E. Elias,¹¹ E. Engels, Jr.,³⁴ R. Erbacher,¹¹ D. Errede,¹⁸ S. Errede,¹⁸ Q. Fan,³⁶ R. G. Feild,⁴⁷ J. P. Fernandez,¹¹ C. Ferretti,³³ R. D. Field,¹² I. Fiori,³ B. Flaughier,¹¹ G. W. Foster,¹¹ M. Franklin,¹⁶ J. Freeman,¹¹ J. Friedman,²⁴ Y. Fukui,²² I. Furic,²⁴ S. Galeotti,³³ A. Gallas,(**)¹⁶ M. Gallinaro,³⁷ T. Gao,³² M. Garcia-Sciveres,²³ A. F. Garfinkel,³⁵ P. Gatti,³¹ C. Gay,⁴⁷ D. W. Gerdes,²⁵ P. Giannetti,³³ P. Giromini,¹³ V. Glagolev,⁹ D. Glenzinski,¹¹ M. Gold,²⁷ J. Goldstein,¹¹ I. Gorelov,²⁷ A. T. Goshaw,¹⁰ Y. Gotra,³⁴ K. Goulianatos,³⁷ C. Green,³⁵ G. Grim,⁵ P. Gris,¹¹ L. Groer,³⁸ C. Grossi-Pilcher,⁸ M. Guenther,³⁵ G. Guillian,²⁵ J. Guimaraes da Costa,¹⁶ R. M. Haas,¹² C. Haber,²³ S. R. Hahn,¹¹ C. Hall,¹⁶ T. Handa,¹⁷ R. Handler,⁴⁶ W. Hao,⁴⁰ F. Happacher,¹³ K. Hara,⁴³ A. D. Hardman,³⁵ R. M. Harris,¹¹ F. Hartmann,²⁰ K. Hatakeyama,³⁷ J. Hauser,⁶ J. Heinrich,³² A. Heiss,²⁰ M. Herndon,¹⁹ C. Hill,⁵ K. D. Hoffman,³⁵ C. Holck,³² R. Hollebeek,³² L. Holloway,¹⁸ R. Hughes,²⁸ J. Huston,²⁶ J. Huth,¹⁶ H. Ikeda,⁴³ J. Incandela,¹¹ G. Introzzi,³³ J. Iwai,⁴⁵ Y. Iwata,¹⁷ E. James,²⁵ M. Jones,³² U. Joshi,¹¹ H. Kambara,¹⁴ T. Kamon,³⁹ T. Kaneko,⁴³ K. Karr,⁴⁴ H. Kasha,⁴⁷ Y. Kato,²⁹ T. A. Keaffaber,³⁵ K. Kelley,²⁴ M. Kelly,²⁵ R. D. Kennedy,¹¹ R. Kephart,¹¹ D. Khazins,¹⁰ T. Kikuchi,⁴³ B. Kilminster,³⁶ B. J. Kim,²¹ D. H. Kim,²¹ H. S. Kim,¹⁸ M. J. Kim,²¹ S. B. Kim,²¹ S. H. Kim,⁴³ Y. K. Kim,²³ M. Kirby,¹⁰ M. Kirk,⁴ L. Kirsch,⁴ S. Klimentko,¹² P. Koehn,²⁸ K. Kondo,⁴⁵ J. Konigsberg,¹² A. Korn,²⁴ A. Korytov,¹² A. V. Kotwal,¹⁰ E. Kovacs,² J. Kroll,³² M. Kruse,¹⁰ S. E. Kuhlmann,² K. Kurino,¹⁷ T. Kuwabara,⁴³ A. T. Laasanen,³⁵ N. Lai,⁸ S. Lami,³⁷ S. Lammel,¹¹ J. Lancaster,¹⁰ M. Lancaster,²³ R. Lander,⁵ A. Lath,³⁸ G. Latino,³³ T. LeCompte,² A. M. Lee IV,¹⁰ K. Lee,⁴⁰ S. Leone,³³ J. D. Lewis,¹¹

M. Lindgren,⁶ T. M. Liss,¹⁸ J. B. Liu,³⁶ Y. C. Liu,¹ D. O. Litvintsev,¹¹ O. Lobban,⁴⁰
 N. Lockyer,³² J. Loken,³⁰ M. Loreti,³¹ D. Lucchesi,³¹ P. Lukens,¹¹ S. Lusin,⁴⁶ L. Lyons,³⁰
 J. Lys,²³ R. Madrak,¹⁶ K. Maeshima,¹¹ P. Maksimovic,¹⁶ L. Malferrari,³ M. Mangano,³³
 M. Mariotti,³¹ G. Martignon,³¹ A. Martin,⁴⁷ J. A. J. Matthews,²⁷ J. Mayer,⁴¹ P. Mazzanti,³
 K. S. McFarland,³⁶ P. McIntyre,³⁹ E. McKigney,³² M. Menguzzato,³¹ A. Menzione,³³
 C. Mesropian,³⁷ A. Meyer,¹¹ T. Miao,¹¹ R. Miller,²⁶ J. S. Miller,²⁵ H. Minato,⁴³ S. Miscetti,¹³
 M. Mishina,²² G. Mitselmakher,¹² N. Moggi,³ E. Moore,²⁷ R. Moore,²⁵ Y. Morita,²²
 T. Moulik,³⁵ M. Mulhearn,²⁴ A. Mukherjee,¹¹ T. Muller,²⁰ A. Munar,³³ P. Murat,¹¹
 S. Murgia,²⁶ J. Nachtman,⁶ V. Nagaslaev,⁴⁰ S. Nahn,⁴⁷ H. Nakada,⁴³ I. Nakano,¹⁷
 C. Nelson,¹¹ T. Nelson,¹¹ C. Neu,²⁸ D. Neuberger,²⁰ C. Newman-Holmes,¹¹ C.-Y. P. Ngan,²⁴
 H. Niu,⁴ L. Nodulman,² A. Nomerotski,¹² S. H. Oh,¹⁰ Y. D. Oh,²¹ T. Ohmoto,¹⁷
 T. Ohsugi,¹⁷ R. Oishi,⁴³ T. Okusawa,²⁹ J. Olsen,⁴⁶ W. Orejudos,²³ C. Pagliarone,³³
 F. Palmonari,³³ R. Paoletti,³³ V. Papadimitriou,⁴⁰ D. Partos,⁴ J. Patrick,¹¹ G. Pauletta,⁴²
 M. Paulini,(*)²³ C. Paus,²⁴ D. Pellett,⁵ L. Pescara,³¹ T. J. Phillips,¹⁰ G. Piacentino,³³
 K. T. Pitts,¹⁸ A. Pompos,³⁵ L. Pondrom,⁴⁶ G. Pope,³⁴ M. Popovic,⁴¹ F. Prokoshin,⁹
 J. Proudfoot,² F. Ptahos,¹³ O. Pukhov,⁹ G. Punzi,³³ A. Rakitine,²⁴ F. Ratnikov,³⁸
 D. Reher,²³ A. Reichold,³⁰ A. Ribon,³¹ W. Riegler,¹⁶ F. Rimondi,³ L. Ristori,³³ M. Riveline,⁴¹
 W. J. Robertson,¹⁰ A. Robinson,⁴¹ T. Rodrigo,⁷ S. Rolli,⁴⁴ L. Rosenson,²⁴ R. Roser,¹¹
 R. Rossin,³¹ C. Rott,³⁵ A. Roy,³⁵ A. Ruiz,⁷ A. Safonov,⁵ R. St. Denis,¹⁵ W. K. Sakumoto,³⁶
 D. Saltzberg,⁶ C. Sanchez,²⁸ A. Sansoni,¹³ L. Santi,⁴² H. Sato,⁴³ P. Savard,⁴¹ P. Schlabach,¹¹
 E. E. Schmidt,¹¹ M. P. Schmidt,⁴⁷ M. Schmitt,(**)¹⁶ L. Scodellaro,³¹ A. Scott,⁶ A. Scribano,³³
 S. Segler,¹¹ S. Seidel,²⁷ Y. Seiya,⁴³ A. Semenov,⁹ F. Semeria,³ T. Shah,²⁴ M. D. Shapiro,²³
 P. F. Shepard,³⁴ T. Shibayama,⁴³ M. Shimojima,⁴³ M. Shochet,⁸ A. Sidoti,³¹ J. Siegrist,²³
 A. Sill,⁴⁰ P. Sinervo,⁴¹ P. Singh,¹⁸ A. J. Slaughter,⁴⁷ K. Sliwa,⁴⁴ C. Smith,¹⁹ F. D. Snider,¹¹
 A. Solodsky,³⁷ J. Spalding,¹¹ T. Speer,¹⁴ P. Spicas,²⁴ F. Spinella,³³ M. Spiropulu,¹⁶
 L. Spiegel,¹¹ J. Steele,⁴⁶ A. Stefanini,³³ J. Strologas,¹⁸ F. Strumia,¹⁴ D. Stuart,¹¹
 K. Sumorok,²⁴ T. Suzuki,⁴³ T. Takano,²⁹ R. Takashima,¹⁷ K. Takikawa,⁴³ P. Tamburello,¹⁰
 M. Tanaka,⁴³ B. Tannenbaum,⁶ M. Tecchio,²⁵ R. Tesarek,¹¹ P. K. Teng,¹ K. Terashi,³⁷
 S. Tether,²⁴ A. S. Thompson,¹⁵ R. Thurman-Keup,² P. Tipton,³⁶ S. Tkaczyk,¹¹ D. Toback,³⁹
 K. Tollefson,³⁶ A. Tollestrup,¹¹ D. Tonelli,³³ H. Toyoda,²⁹ W. Trischuk,⁴¹ J. F. de Troconiz,¹⁶
 J. Tseng,²⁴ N. Turini,³³ F. Ukegawa,⁴³ T. Vaiciulis,³⁶ J. Valls,³⁸ S. Vejcik III,¹¹ G. Velev,¹¹
 G. Veramendi,²³ R. Vidal,¹¹ I. Vila,⁷ R. Vilar,⁷ I. Volobouev,²³ M. von der Mey,⁶ D. Vucinic,²⁴
 R. G. Wagner,² R. L. Wagner,¹¹ N. B. Wallace,³⁸ Z. Wan,³⁸ C. Wang,¹⁰ M. J. Wang,¹
 B. Ward,¹⁵ S. Waschke,¹⁵ T. Watanabe,⁴³ D. Waters,³⁰ T. Watts,³⁸ R. Webb,³⁹ H. Wenzel,²⁰
 W. C. Wester III,¹¹ A. B. Wicklund,² E. Wicklund,¹¹ T. Wilkes,⁵ H. H. Williams,³²
 P. Wilson,¹¹ B. L. Winer,²⁸ D. Winn,²⁵ S. Wolbers,¹¹ D. Wolinski,²⁵ J. Wolinski,²⁶
 S. Wolinski,²⁵ S. Worm,²⁷ X. Wu,¹⁴ J. Wyss,³³ W. Yao,²³ G. P. Yeh,¹¹ P. Yeh,¹ J. Yoh,¹¹
 C. Yosef,²⁶ T. Yoshida,²⁹ I. Yu,²¹ S. Yu,³² Z. Yu,⁴⁷ A. Zanetti,⁴² F. Zetti,²³ and S. Zucchelli³

(CDF Collaboration)

¹ Institute of Physics, Academia Sinica, Taipei, Taiwan 11529, Republic of China

² Argonne National Laboratory, Argonne, Illinois 60439

³ Istituto Nazionale di Fisica Nucleare, University of Bologna, I-40127 Bologna, Italy

- ⁴ Brandeis University, Waltham, Massachusetts 02254
⁵ University of California at Davis, Davis, California 95616
⁶ University of California at Los Angeles, Los Angeles, California 90024
⁷ Instituto de Fisica de Cantabria, CSIC-University of Cantabria, 39005 Santander, Spain
⁸ Enrico Fermi Institute, University of Chicago, Chicago, Illinois 60637
⁹ Joint Institute for Nuclear Research, RU-141980 Dubna, Russia
¹⁰ Duke University, Durham, North Carolina 27708
¹¹ Fermi National Accelerator Laboratory, Batavia, Illinois 60510
¹² University of Florida, Gainesville, Florida 32611
¹³ Laboratori Nazionali di Frascati, Istituto Nazionale di Fisica Nucleare, I-00044 Frascati, Italy
¹⁴ University of Geneva, CH-1211 Geneva 4, Switzerland
¹⁵ Glasgow University, Glasgow G12 8QQ, United Kingdom
¹⁶ Harvard University, Cambridge, Massachusetts 02138
¹⁷ Hiroshima University, Higashi-Hiroshima 724, Japan
¹⁸ University of Illinois, Urbana, Illinois 61801
¹⁹ The Johns Hopkins University, Baltimore, Maryland 21218
²⁰ Institut für Experimentelle Kernphysik, Universität Karlsruhe, 76128 Karlsruhe, Germany
²¹ Center for High Energy Physics: Kyungpook National University, Taegu 702-701; Seoul National University, Seoul 151-742; and SungKyunKwan University, Suwon 440-746; Korea
²² High Energy Accelerator Research Organization (KEK), Tsukuba, Ibaraki 305, Japan
²³ Ernest Orlando Lawrence Berkeley National Laboratory, Berkeley, California 94720
²⁴ Massachusetts Institute of Technology, Cambridge, Massachusetts 02139
²⁵ University of Michigan, Ann Arbor, Michigan 48109
²⁶ Michigan State University, East Lansing, Michigan 48824
²⁷ University of New Mexico, Albuquerque, New Mexico 87131
²⁸ The Ohio State University, Columbus, Ohio 43210
²⁹ Osaka City University, Osaka 588, Japan
³⁰ University of Oxford, Oxford OX1 3RH, United Kingdom
³¹ Universita di Padova, Istituto Nazionale di Fisica Nucleare, Sezione di Padova, I-35131 Padova, Italy
³² University of Pennsylvania, Philadelphia, Pennsylvania 19104
³³ Istituto Nazionale di Fisica Nucleare, University and Scuola Normale Superiore of Pisa, I-56100 Pisa, Italy
³⁴ University of Pittsburgh, Pittsburgh, Pennsylvania 15260
³⁵ Purdue University, West Lafayette, Indiana 47907
³⁶ University of Rochester, Rochester, New York 14627
³⁷ Rockefeller University, New York, New York 10021
³⁸ Rutgers University, Piscataway, New Jersey 08855
³⁹ Texas A&M University, College Station, Texas 77843
⁴⁰ Texas Tech University, Lubbock, Texas 79409
⁴¹ Institute of Particle Physics, University of Toronto, Toronto M5S 1A7, Canada
⁴² Istituto Nazionale di Fisica Nucleare, University of Trieste/ Udine, Italy
⁴³ University of Tsukuba, Tsukuba, Ibaraki 305, Japan
⁴⁴ Tufts University, Medford, Massachusetts 02155
⁴⁵ Waseda University, Tokyo 169, Japan
⁴⁶ University of Wisconsin, Madison, Wisconsin 53706
⁴⁷ Yale University, New Haven, Connecticut 06520

(*) Now at Carnegie Mellon University, Pittsburgh, Pennsylvania 15213

(**) Now at Northwestern University, Evanston, Illinois 60208

Abstract

We present searches for quark-lepton compositeness and a heavy W' boson at high electron-neutrino transverse mass. We use $\sim 110 \text{ pb}^{-1}$ of data collected in $p\bar{p}$ collisions at $\sqrt{s} = 1.8 \text{ TeV}$ by the CDF collaboration during 1992–95. The data are consistent with standard model expectations. Limits are set on the quark-lepton compositeness scale Λ and the ratio of partial cross sections $\sigma(W' \rightarrow e\nu)/\sigma(W \rightarrow e\nu)$. The cross section ratio is used to obtain a lower limit on the mass of a W' boson with standard model couplings. We exclude $\Lambda < 2.81 \text{ TeV}$ and a W' boson with mass below $754 \text{ GeV}/c^2$ at the 95% confidence level. We combine the W' mass limit with our previously published limit obtained using the muon channel, to exclude a W' boson with mass below $786 \text{ GeV}/c^2$ at the 95% confidence level.

The standard model (SM) gives a good description of nature in terms of the fundamental fermions and their interactions via gauge bosons. However, the SM is not expected to be a complete theory. For example, it does not explain the number of fermion families or their mass hierarchy. It also does not provide a unified description of all gauge symmetries. Compositeness models postulate constituents of the SM fermions and new strong dynamics that bind these constituents [1]. Other extensions of the SM postulate larger gauge groups and therefore new forces associated with additional charged gauge bosons, which we generically call W' . For instance, the left-right symmetric model [2] expands the $SU(2)_L \times U(1)$ electroweak group to $SU(2)_L \times SU(2)_R \times U(1)$, predicting an additional right-handed charged gauge boson.

At center-of-mass energies much smaller than the compositeness energy scale Λ , interactions between composite quarks and/or leptons have been parameterized by effective four-fermion contact interactions [1]. Atomic parity violation experiments have set stringent, though model-dependent limits on quark-lepton compositeness in the neutral current channel [3]. Direct searches have set limits on Λ in the range 2.5–6.1 TeV [4–6] in a broad class of neutral current models. In this Letter, we present the first results of a search for compositeness in the charged current channel ($q\bar{q}'e\nu$) using the $e\nu$ final state.

The $e\nu$ final state is also sensitive to the direct production and decay of a W' boson. Previous indirect searches based on μ decay, the $K_L - K_S$ mass difference, neutrinoless double beta decay, and studies of b particles have resulted in stringent model-dependent limits on possible W' bosons [7]. Direct searches in various decay modes have produced lower limits on the W' mass, $m_{W'}$. The best limit of $m_{W'} > 720$ GeV/c² in the $W' \rightarrow e\nu$ channel [8] assumes a light and stable neutrino, standard model couplings for the W' to fermions, and suppressed $W' \rightarrow WZ$ decays, as in extended gauge models [9]. In this Letter, we set upper limits on the ratio of partial cross sections $\sigma(W' \rightarrow e\nu)/\sigma(W \rightarrow e\nu)$ under the same assumptions. We use the latter to obtain the most stringent lower limit on $m_{W'}$. We also present the combined W' mass limit with our previously published limit obtained using the muon channel [10].

We use ~ 110 pb⁻¹ of data collected in $p\bar{p}$ collisions at $\sqrt{s} = 1.8$ TeV by the Collider Detector at Fermilab [11] during 1992–95. The detector includes a tracking system immersed in a 1.4 T magnetic field, scintillator-based sampling electromagnetic and hadronic calorimeters, and a muon detector. For this analysis, electron candidates are accepted in the pseudorapidity range $0.05 < |\eta| < 1.0$, where $\eta = -\log \tan(\theta/2)$, and θ is the polar angle with respect to the beam axis. Electrons detected near the fiducial edges of the calorimeter are removed to ensure uniform calorimeter response. We use a combination of electron and neutrino triggers to obtain an efficiency exceeding 99% for the high transverse mass $e\nu$ final states that pass our offline selection criteria.

After offline reconstruction, the electromagnetic calorimeter cluster with the highest transverse energy ($E_T \equiv E \sin \theta$) in the event must satisfy these requirements: (i) the electron must deposit most [12] of its energy in the electromagnetic calorimeter, (ii) a track in the central drift chamber must match the calorimeter cluster in position, (iii) the electron must be isolated in a cone of radius $R \equiv \sqrt{\Delta\eta^2 + \Delta\phi^2} = 0.4$, such that the fractional excess transverse energy in the cone, $\frac{E_T^{tot}(R=0.4) - E_T^e}{E_T^e} < 0.1$, where E_T^{tot} and E_T^e are the total and electron transverse energies respectively. The kinematic cuts used to define the data sample

are $E_T^e > 30$ GeV, the transverse momentum (p_T) of the associated track $p_T^e > 13$ GeV/c, the missing transverse energy $\cancel{E}_T > 30$ GeV, and the electron-neutrino transverse mass $m_T(e\nu) > 50$ GeV/c 2 , where $m_T(e\nu) = \sqrt{2 E_T^e \cancel{E}_T (1 - \cos \phi_{e\nu})}$, and $\phi_{e\nu}$ is the azimuthal angle between the electron and the \cancel{E}_T direction. The neutrino transverse momentum is identified with \cancel{E}_T by requiring transverse momentum balance in the event. Electron identification cuts based on E/p (ratio of calorimeter energy to matched track momentum) and calorimeter energy profiles, which are imposed for $E_T^e < 50$ GeV to suppress jet misidentification backgrounds, are released for $E_T^e > 50$ GeV to ensure maximum signal efficiency. A total of 31,436 events pass our selection criteria.

We use the PYTHIA [13] program to compute the compositeness and W' signal processes. The detector response is simulated using a parameterized Monte Carlo program. The electromagnetic calorimeter sampling term is derived from test beam data. The underlying event contribution to the electron energy resolution is derived from $W \rightarrow e\nu$ collider data. The constant term in the electromagnetic resolution is tuned to reproduce the observed width of the $Z \rightarrow ee$ mass peak. The electromagnetic energy scale is set so that the reconstructed Z boson mass agrees with the world-average Z mass [14]. The hadronic response and resolution are tuned by studying the p_T balance in $Z \rightarrow ee$ events.

In this analysis we normalize the number of SM background Monte Carlo events after detector simulation to the large inclusive W boson sample in the data. Thus we are analysing the shape of the $e\nu$ transverse mass distribution, and are insensitive to the uncertainty in the integrated luminosity of the data and to the overall efficiency. The efficiency of the additional electron identification cuts applied for $E_T^e < 50$ GeV is determined using $Z \rightarrow ee$ data where one of the electrons is tagged. The second electron then provides an unbiased sample with which to measure the efficiencies. Background subtraction is performed using the sidebands of the Z boson mass distribution. The combined efficiency of these additional cuts is $(95.8 \pm 0.3)\%$, relative to the full efficiency at high E_T^e .

The most important sources of misidentification background to $p\bar{p} \rightarrow e\nu + X$ are (i) QCD multijet events, where a jet is misidentified as an electron and there is sufficient energy mismeasurement to create significant \cancel{E}_T , and (ii) $Z \rightarrow ee$ events where one electron is lost or misreconstructed. The electromagnetic energy in a jet which has been misidentified as an electron is likely to be non-isolated. We select a representative sample of misidentified electrons by making the electron identification cuts on the base sample without the isolation cut, and then selecting non-isolated candidates. The relative normalization of this sample to the jet background in the signal sample is obtained from a “pure-jet” sample. The “pure-jet” sample is obtained in the same way as the signal sample except $\cancel{E}_T < 10$ GeV, which excludes almost all W events. This technique assumes that the isolation for a jet is independent of \cancel{E}_T . The systematic uncertainty of 30% on the jet misidentification background is estimated by studying the correlation between isolation and \cancel{E}_T . The $Z \rightarrow ee$ background is estimated using a Monte Carlo sample of $Z \rightarrow ee$ events, passed through a full detector simulation and reconstructed like the data. The systematic uncertainty of 23% on the $Z \rightarrow ee$ background is estimated by varying the detector response to electrons near the fiducial edges of the calorimeter. Other systematic uncertainties, indicated in Table II, are derived by varying the parameters in the Monte Carlo simulation. The uncertainty due to parton distribution functions is taken to be identical with our published $W' \rightarrow \mu\nu$ analysis [10].

TABLE I. The observed number of events and the total expected number of events from SM and detector background sources, in transverse mass bins.

m_T bin (GeV/c^2)	N_{observed}	N_{expected}
150-200	70	62.2 ± 8.5
200-250	18	18.3 ± 3.4
250-300	5	4.01 ± 0.44
300-350	2	1.61 ± 0.18
350-400	0	0.72 ± 0.08
400-500	1	0.49 ± 0.06
500-600	0	0.11 ± 0.02
600-1000	0	0.05 ± 0.01

Other high p_T processes also contribute to $e\nu$ final states. Using PYTHIA, we evaluate the following background processes, $W \rightarrow e\nu$ (dominant), $W \rightarrow \tau\nu \rightarrow e\nu X$, $t\bar{t} \rightarrow e\nu X$, $WW \rightarrow e\nu X$, $WZ \rightarrow e\nu X$, $ZZ \rightarrow e\nu X$ and $\gamma^*/Z \rightarrow \tau\tau \rightarrow e\nu X$. We pass these Monte Carlo events through the parameterized detector simulation to estimate their contribution. These physics backgrounds dominate over the misidentification backgrounds at high $e\nu$ transverse mass, due to the presence of real neutrino(s) producing large \cancel{E}_T . For example, the jet and $Z \rightarrow ee$ misidentification background fractions amount to 25% and 3% respectively for $m_T(e\nu) > 150 \text{ GeV}/c^2$.

TABLE II. Systematic uncertainties on the SM background and the signal due to the parton distribution functions (PDFs), the K -factor, and the detector model.

	SM Background (%)	Signal (%)
PDFs	10	10
K -factor	4	4
hadronic resolution	0.1	2
vertex z width	0.5	1.8
hadronic scale	0.2	1.6
EM resolution	0.1	1.5
electron efficiency	1.0	1.0
EM scale	0.2	0.9
total	11	12

Figure 1 shows the transverse mass distribution of the data events normalized to the bin width. Also shown is the expectation based on SM processes and detector backgrounds. We apply a mass-dependent K -factor (defined as the ratio of the next-to-next-to leading order (NNLO) and the leading-order (LO) Drell-Yan cross section calculations from Ref. [15]) to the LO PYTHIA calculation. The K -factor varies between 1.24 at $80 \text{ GeV}/c^2$ and 1.65 at $800 \text{ GeV}/c^2$. The effects of the detector acceptance and response have been folded into the theoretical prediction. Table I shows the expected and the observed number of events in the

high transverse mass bins. There is good agreement between the data and the expectation. Also shown are all backgrounds excluding the dominant SM $W \rightarrow e\nu$ process, and the expectation of the compositeness model with $\Lambda = 2$ TeV.

To set a limit on the compositeness scale Λ , we generate Monte Carlo events for the compositeness process using PYTHIA, corrected with the K -factor. We perform a Bayesian analysis [14] of the shape of the m_T distribution of events. The expected number of events in the k^{th} transverse mass bin is denoted by $N_\Lambda^k = b^k + \mathcal{L}\epsilon^k\sigma_\Lambda^k$, where σ_Λ^k is the predicted cross section for a given scale Λ , and ϵ^k and b^k denote the total acceptance and remaining backgrounds in the k^{th} bin. The prediction for the number of events, including all backgrounds, is normalized to the observed number of events for $m_T(e\nu) < 150$ GeV/c². Given the data (D), we compute the posterior probability distribution for Λ according to

$$P(\Lambda|D) = \frac{1}{A} \int db d\epsilon \prod_{k=1}^n \left[\frac{e^{-N_\Lambda^k} N_\Lambda^{N_o^k}}{N_o^k!} P(b^k, \epsilon^k) \right] P(\Lambda).$$

N_o^k denotes the observed number of events. We take the prior distribution $P(b^k, \epsilon^k)$ of the nuisance parameters b and ϵ to be Gaussian with the r.m.s. given by their total uncertainties. The bin-to-bin correlations in the uncertainty on the acceptance and background are taken into account. We make the conventional choice for the prior distribution $P(\Lambda)$ to be uniform in $1/\Lambda^2$. The 95% C.L. lower limit is defined by $\int_\Lambda^\infty P(\Lambda'|D)d\Lambda' = 0.95$, yielding $\Lambda > 2.81$ TeV. The expected limit, obtained when the observed number of events is set equal to the expected number, is $\Lambda > 2.70$ TeV. Varying the choice of the prior distribution $P(\Lambda)$ changes the limit by 10%.

To set a limit on the mass of a W' boson, we compute the Poisson probability for the observed number of events given $N_{\text{expected}} = N_{\text{background}} + N_{W'}$. The Poisson probability is computed separately in three search windows: $0.5M_{W'} < m_T < 0.65M_{W'}$, $0.65M_{W'} < m_T < 0.8M_{W'}$ and $0.8M_{W'} < m_T < 1.1M_{W'}$, and then the probabilities are combined. The use of three windows allows us to exploit the difference in the shape of the W' signal and background m_T distributions. Uncertainties in the backgrounds and signal acceptance are incorporated by convoluting the probability $P(N_{W'})$ over Gaussian fluctuations in these parameters, taking correlations across bins into account. The 95% C.L. upper limit on the number of W' signal events, $N_{W'}^{95}$, is defined by $\int_0^{N_{W'}^{95}} P(N_{W'})d(N_{W'}) = 0.95$. The limit $N_{W'}^{95}$ may be expressed as a 95% C.L. limit on the ratio $\sigma B(W' \rightarrow e\nu)/\sigma B(W \rightarrow e\nu)$ using

$$\left(\frac{\sigma B(W' \rightarrow e\nu)}{\sigma B(W \rightarrow e\nu)} \right)_{95} = \frac{N_{W'}^{95} A_{W'}}{A_{W'} N_W}$$

where N_W is the observed number of SM W events and $A_{W'}(A_W)$ is the total acceptance for $W' \rightarrow e\nu$ ($W \rightarrow e\nu$) decays. The 95% C.L. upper limit on $\sigma B(W' \rightarrow e\nu)/\sigma B(W \rightarrow e\nu)$ is plotted as a function of $M_{W'}$ in Fig. 2 together with the theory curve from PYTHIA 6.129, assuming standard model couplings and including the K -factor. From the intersection of the two curves, a W' boson with mass $m_{W'} < 754$ GeV/c² is excluded at 95% C.L. The expected limit in this case is 748 GeV/c². We combine this result with our previously published result on a W' boson using the $\mu\nu$ final state [10]. Taking the PDF uncertainty to be fully correlated between the two analyses and with the same model assumptions, we obtain the combined limit excluding $m_{W'} < 786$ GeV/c² at the 95% C.L.

In conclusion, we find no significant deviation between the measured $e\nu$ transverse mass distribution at high transverse mass and the SM prediction. We have used the data to exclude the quark-lepton compositeness scale $\Lambda < 2.81$ TeV, in the context of an effective contact interaction. We set limits on the ratio of the cross section times branching ratio to $e\nu$ of a W' boson to a standard model W boson. We use the latter to exclude a W' boson with SM couplings and mass $m_{W'} < 754$ GeV/c². Combining with our muon channel result, we exclude $m_{W'} < 786$ GeV/c² at the 95% C.L.

We thank T. Sjöstrand for discussions regarding PYTHIA and W. L. Van Neerven for providing the code to compute the NNLO SM Drell-Yan cross section. We thank the Fermilab staff and the technical staffs of the participating institutions for their vital contributions. This work was supported by the U.S. Department of Energy and National Science Foundation; the Italian Istituto Nazionale di Fisica Nucleare; the Ministry of Education, Science, Sports and Culture of Japan; the Natural Sciences and Engineering Research Council of Canada; the National Science Council of the Republic of China; the Swiss National Science Foundation; the A. P. Sloan Foundation; the Bundesministerium fuer Bildung und Forschung, Germany; the Korea Science and Engineering Foundation (KoSEF); the Korea Research Foundation; and the Comision Interministerial de Ciencia y Tecnologia, Spain.

REFERENCES

- [1] E. Eichten, K. Lane and M. Peskin, Phys. Rev. Lett. **50**, 811 (1983) and references therein; E. Eichten, I. Hinchliffe, K. Lane and C. Quigg, Rev. Mod. Phys. **56**, 579 (1984) and references therein.
- [2] R. N. Mohapatra, *Unification and Supersymmetry*, (Springer, New York, 1992), and references therein.
- [3] C. S. Wood *et al.*, Science **275**, 1759 (1997); P. Langacker, Phys. Lett. B **256**, 277 (1991); M. Leurer, Phys. Rev. D **49**, 333 (1994).
- [4] DØ Collaboration, B. Abbott *et al.*, Phys. Rev. Lett. **82**, 4769 (1999).
- [5] CDF Collaboration, F. Abe *et al.*, Phys. Rev. Lett. **79**, 2198 (1997).
- [6] OPAL Collaboration, K. Ackerstaff *et al.*, Phys. Lett. B **391**, 221 (1997).
- [7] P. Langacker and S. U. Sankar, Phys. Rev. D **40**, 1569 (1989), and references therein.
- [8] DØ Collaboration, S. Abachi *et al.*, Phys. Rev. Lett. **76**, 3271 (1996).
- [9] G. Altarelli *et al.*, Z. Phys. C **45**, 109 (1989), Erratum-ibid. C **47**, 676 (1990), and references therein; P. Ramond, Ann. Rev. Nucl. Part. Sci. **33**, 31 (1983) and references therein.
- [10] CDF Collaboration, F. Abe *et al.*, Phys. Rev. Lett. **84**, 5716 (2000).
- [11] CDF Collaboration, F. Abe *et al.*, Nucl. Instrum. Methods Phys. Res. A **271**, 387 (1988); D. Amidei *et al.*, Nucl. Instrum. Methods Phys. Res. A **350**, 73 (1994).
- [12] For electron candidates we require $E_{had}/E_{em} < 0.055 + 0.045 \times (E^e / 100 \text{ GeV})$, where E_{had} and E_{em} are the hadronic and electromagnetic energies respectively.
- [13] PYTHIA version 6.129, T. Sjöstrand, Comp. Phys. Commun. **82**, 74 (1994).
- [14] Particle Data Group, D. E. Groom *et al.*, Eur. Phys. J. C **15**, 1 (2000).
- [15] R. Hamberg, W. L. Van Neerven and T. Matsuura, Nucl. Phys. B **359**, 343 (1991).

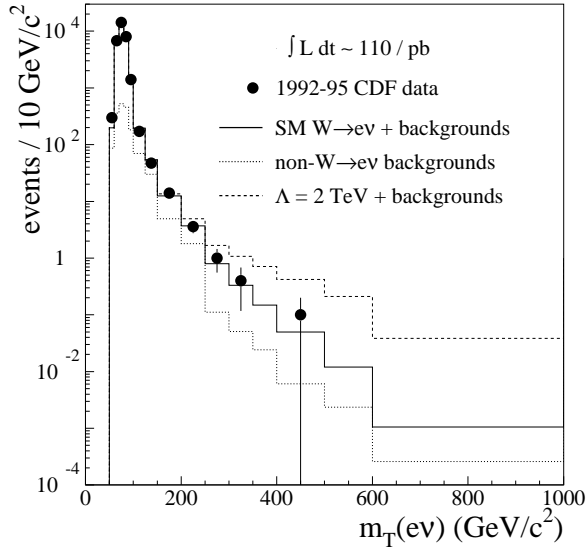


FIG. 1. The event yield from the data as a function of the $e\nu$ transverse mass, normalized to the bin width. Also shown are the SM prediction including backgrounds, all backgrounds excluding the dominant SM $W \rightarrow e\nu$ process, and the prediction of the compositeness process with energy scale $\Lambda = 2$ TeV. The simulation of the physics processes includes the effects of detector acceptance and response.

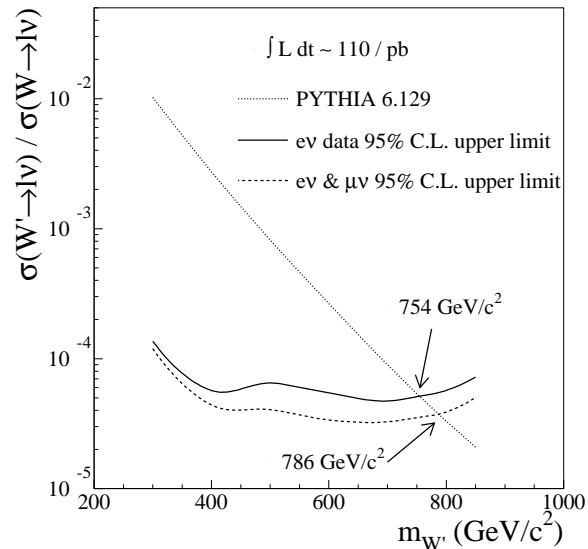


FIG. 2. The 95% C.L. upper limit on the ratio of partial cross sections $\sigma(W' \rightarrow \ell\nu)/\sigma(W \rightarrow \ell\nu)$, for the e data and the combined $e + \mu$ data. Also shown is the SM prediction for this ratio, and the $m_{W'}$ limits obtained from the intersection of the experimental and theory curves.